Materials Research Letters

ISSN: (Print) (Online) Journal homepage: https://www.tandfonline.com/loi/tmrl20

N-doped carbon materials as electrodes for highly stable supercapacitors

Anna Ilnicka, Malgorzata Skorupska, Mariusz Szkoda, Zuzanna Zarach & Jerzy P. Lukaszewicz

To cite this article: Anna Ilnicka, Malgorzata Skorupska, Mariusz Szkoda, Zuzanna Zarach & Jerzy P. Lukaszewicz (2023) N-doped carbon materials as electrodes for highly stable supercapacitors, Materials Research Letters, 11:3, 213-221, DOI: 10.1080/21663831.2022.2139163

To link to this article: https://doi.org/10.1080/21663831.2022.2139163

MATER. RES. LETT.
2023, VOL. 11, NO. 3, 213–221
https://doi.org/10.1080/21663831.2022.2139163

MATERIALS RESEARCH LETTERS
Taylor & Francis
Taylor & Francis Group

ORIGINAL REPORTS

N-doped carbon materials as electrodes for highly stable supercapacitors

Anna Ilnicka[a], Malgorzata Skorupska[a], Mariusz Szkoda[b,c], Zuzanna Zarach[b] and Jerzy P. Lukaszewicz[a,d]

[a]Faculty of Chemistry, Nicolaus Copernicus University in Torun, Torun, Poland; [b]Faculty of Chemistry, Department of Chemistry and Technology of Functional Materials, Gdańsk University of Technology, Gdańsk, Poland; [c]Advanced Materials Center, Gdańsk University of Technology, Gdańsk, Poland; [d]Centre for Modern Interdisciplinary Technologies, Nicolaus Copernicus University in Torun, Torun, Poland

ABSTRACT

This article reports a strategy to use nitrogen-doped carbon materials as electrodes for supercapacitors. Depending on the carbon precursor, the porous structure is changed with specific surface area reached up to 2270 $m^2 g^{-1}$. The capacitance of carbon materials used as electrodes is related strictly to pore size. The microstructure and nitrogen functionalities enable a high capacitance (327 $F g^{-1}$) and cycle durability. The nanoporous carbon electrode exhibits long-term cycle life and high cycle stability with a retention of 86% of its initial after 10,000 cycles in neutral electrolyte. Highly porous carbons are thus considered a promising material for supercapacitors.

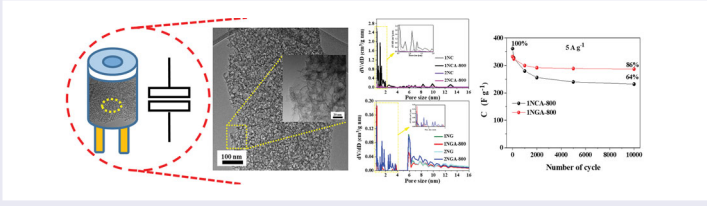

ARTICLE HISTORY
Received 15 August 2022

KEYWORDS
Carbon electrode; porous structure; high stability; supercapacitor

1. Introduction

Recently, composite carbon materials have become a subject of special interest as potential electrode materials for batteries and energy storage devices [1,2]. Composites with transition-metal oxides were investigated as alternative materials for supercapacitor electrodes to improve the specific capacitance and the energy density [3,4], however, due to their high price, composites and hybrids with heteroatoms have also been studied [5–7]. Recent reports demonstrate that doping nitrogen onto the surface of carbon gives rise to charge delocalization and thereby facilitates selective adsorption and transfer [8,9]. In general, nitrogen doping can be achieved through post-treatment with small molecular agents such as urea, melamine, and ammonia gas [10–13]. Some recent research also suggests that heteroatom doping can increase the conductivity of porous carbon materials [14,15].

The pivotal and novel idea for forming hybrid materials from carbon nanotubes on a porous carbon surface using the thermal conversion of poly(furfuryl alcohol) was described in our first paper in this field [16]. Recently, we reported a method of preparing activated carbon containing nitrogen using chitin, chitosan, lysine, and green algae as carbon source [17,18]. The obtained materials had many advantages, including their very high nitrogen content; however, treating the carbon surface with furfuryl alcohol reduced the specific surface area. Therefore, to consider the potential use of these carbons in electrochemistry, additional activation processes were required, which were in turn used in the research presented in this publication.

The good performance of a supercapacitor depends on the proper structure of the electrode and also on the content of additional functional groups, which directly affect the transport of ions and also has a positive effect on the load stability of the electrode materials and promote the uniform intensity of the internal electric field. Compared with two-dimensional graphene, carbon nanotubes also 3D materials [19] are used for such devices due to their unique mechanical or electronic properties. The adequate density of carbon nanotubes results in uniform distribution of ionic charge, electric field strength is increased thus improving electrochemical

CONTACT Anna Ilnicka ailnicka@umk.pl Faculty of Chemistry, Nicolaus Copernicus University in Torun, Gagarina 7, 87-100, Torun, Poland

Supplemental data for this article can be accessed here. https://doi.org/10.1080/21663831.2022.2139163

properties. However, once a certain value of nanotube density is exceeded, the opposite effect can be achieved to the expected effect causing a reduction in the capacity/capacitance of the supercapacitor [20]. Limitations that may occur in the use of hybrids containing transition metals are, in addition to price and safe synthesis, one can also mention the difficulty in obtaining the appropriate structure and properties. Therefore, researchers are trying to find solutions that effectively counteract the various limitations [21,22]. The paper described by He et al. [23] presents metal-free structures of porous carbon materials that work effectively in high-performance supercapacitors while showing stability and featuring an uncomplicated synthesis method. The synthesis is based on the formation of nanoporous carbon materials without metal–organic structures (MOFs) which is an attractive approach and can be a major challenge that we have addressed.

In this work, carbon obtained from green algae and gelatin was activated through chemical treatment, using the same amount of activator with carbonization temperature of 800°C. The influence of synthesis conditions on the porous structure was investigated. The structure and properties of the obtained highly porous materials, to be used as supercapacitor electrodes, were evaluated in neutral electrolyte. Both types of prepared electrodes possessed micropores and mesopores. Electrochemical properties dependent on the used type of carbon and electrolyte were identified, such as capacitance and rate performance. It was observed for electric double-layer supercapacitors that low nitrogen content in electrodes is sufficient for efficient energy storage. The porous structure of the electrodes used had the greatest influence on their properties.

2. Materials and methods

2.1. Preparation of carbon materials

Porous carbon materials were synthesized in a templating process using silicon dioxide described in our previous paper [24,25]. The first step of the synthesis procedure is described in the Supplementary Information. In the next step, in order to increase the specific surface area, the obtained materials were mixed with potassium hydroxide in a mass ratio of 1:4. The mass was then carbonized at 800°C in a tube furnace in a N_2 atmosphere at a rate of 10°C min^{-1} and kept there for 1 h. After activation, the samples were washed with distilled water to remove KOH and other impurities until pH stabilized at 7. This was followed by drying at 120°C overnight, eventually producing porous carbons. A series of samples was prepared with carbonization temperature 800°C, and the resultant products were denoted as 1NCA-T, 2NCA-T, and 1NGA-T, 2NGA-T, where A—stands for a carbon material after potassium hydroxide activation, T—stands for the activation temperature denoted as 800 in the samples' names.

2.2. Characterization methods

The morphology of the carbons was characterized using a high-resolution transmission electron microscope (HRTEM, FEI Europe production, Tecnai F20 X-Twin model) with an acceleration voltage of 200 kV. Nitrogen, carbon, and hydrogen content was determined using a CHN VarioElemental analyser. In order to analyse the surface composition of the obtained materials, X-ray photoelectron spectroscopy (XPS) measurements were performed using the PHI5000 VersaProbe II Scanning XPS Microprobe spectrometer with a high-performance monochromatic Al Kα X-ray source. XPS spectra were taken after all binding energies were referenced to the C1s neutral carbon peak at 284.8 eV. Nitrogen adsorption–desorption measurements at −196°C were performed with ASAP2020 Plus, Micromeritics. Before each measurement, a sample was outgassed in a vacuum at 200°C for 24 h. The specific surface area was calculated using the Brunauer–Emmett–Teller (BET) method and pore size distribution was calculated using the density functional theory (DFT) method.

3. Electrochemical measurements

3.1. Three-electrode configuration

The electrode materials were prepared by mixing the active material, carbon black, and poly-vinylidenefluoride (PVDF) with the weight ratio of 8:1:1 in ethanol and then coating the graphite foil current collectors with this mixture. Finally, the fabricated carbon electrodes were dried at 60°C for 24 h. Three-electrode configuration measurements were performed in 0.2 M K_2SO_4 electrolyte with Ag/AgCl (3 M KCl) and platinum mesh as a reference and a counter electrode, respectively. All the electrochemical measurements were carried out on a potentiostat/galvanostat (BioLogic VSP 2078) using cyclic voltammetry (CV) and galvanostatic charge–discharge (GCD). CV of each three-electrode setup was investigated from −1 to +1 V vs. Ag/AgCl (3 M KCl) with a scan rate of $\nu = 50\,mV\,s^{-1}$. GCD was performed in the same potential range at a current density of $j = 3\,mA\,cm^{-2}$.

3.2. Two-electrode configuration with neutral electrolyte

The symmetric two-electrode supercapacitors were assembled using two electrodes with exactly the same mass of the active material, which was coated onto the graphite foil current collectors. The mass loading of the deposited layers of carbon materials ranged from 7.2 to 11 mg cm^{-2} (1NCA-800–7.9 mg cm^{-2}, 2NCA-800–11 mg cm^{-2}, 1NGA-800–9.3 mg cm^{-2}, 2NGA-800–7.2 mg cm^{-2}). A glass fiber separator soaked with 0.2 M K_2SO_4 was placed between the two electrodes, each of them the size of 20 mm × 20 mm. Afterwards, the casing foil was welded on three sides using a plastic foil welder, and finally the setup was sealed using a vacuum packing machine. For the obtained supercapacitors, GCD measurements (1000 cycles) were performed. Electrochemical tests were conducted with current density values in the range of 1–10 A g^{-1}, with the voltage value of 1 V. The equations for calculation of specific capacitance, energy density, and power density can be found in the Supplementary Information. Moreover, EIS was performed for two of the best materials in a frequency range between 20 kHz and 1 Hz with a voltage amplitude of 10 mV at an open circuit potential.

4. Results and discussion

4.1. Materials characterization

The porous structure was observed through HRTEM for both green algae-based and gelatine-based samples, which is depicted in Figure 1. HRTEM images show that carbon samples exhibited a uniform porous structure with a rough surface and a great number of pores of various sizes.

The silicon dioxide was easily removed from all samples; the 1-NC and 2-NC samples (Figure 1(a,b)) exhibit a smaller total pore volume (detailed description of V_t and BET can be found in the Supplementary Information and Table S1) than the 1-NG and 2-NG samples (Figure 1(c,d)), which were characterized by the presence of thinner walls.

A chemical activation process involving carbonization and KOH activation was employed to produce a high specific surface area and highly porous structure. The 1NCA-800 and 2NCA-800 samples after KOH activation had porous surface with variable pore size (Figure S1(a,b)). The figures indicate that the samples had a rough surface with many pores. It is also possible to distinguish cavities on the surface of the 1NGA-800 and 2NGA-800 samples (Figure S1(c,d)).

In general, the surface properties of electrode materials are a crucial factor affecting electrochemical performance and thus the energy storage abilities of carbon materials that store charges through the formation of an electrical double layer (EDL). Figure 2 shows the nitrogen adsorption–desorption isotherms (Figure 2(a,b)) of the N-containing carbons and the calculated pore size distributions (Figure 2(c,d)).

The presented isotherm plots can be described as type IV isotherms with hysteresis loop, suggesting both micro- and mesoporous nature of the samples. The pore size of samples obtained in the NC series (Figure 2(c)) ranges mainly from 0.5 to 2 nm with a high degree of microporosity development and from 2 to 14 nm which confirm the presence also of mesopores. The NG series (Figure 2(d)) the pore size distribution is in the same region as for NC series from 0.5 to 14 nm. It is well known that mesopores play an important role in promoting fast ion adsorption in the bulk of the material [26,27].

An XPS survey was employed to confirm the presence of the elements and the existence of their corresponding forms. One sample from each NG and NC series was selected for analysis; as shown in the survey spectra for the two samples (Figure S2(a,d)), signals of carbon and oxygen were detected. The high-resolution XPS spectra of the C1s and O1s regions are illustrated in Figure S2(b,e) and (c,f), respectively. Both samples 1NCA-800 and 2NGA-800 show similar C and O signals in the XPS spectra. Different binding energies indicate that the C atoms were linked with one O atom by a single bond, or with two O atoms. Detailed information about the deconvolution of C1s and O1s is described in the Supplementary Information. 1NCA-800 shows an oxygen content of 6.5 at.%, while 2NGA-800 has an oxygen content of 9.2 at.%. Because the amount of N-doped cannot be reliably detected in wide scan XPS, we employed combustible elemental analysis to obtain accurate measurements of the concentration of these trace element. The nitrogen content of all samples was identified by elemental analysis (Table S1 in the Supplementary Information). The amounts of N-doped approximately the same for the analysed series, and a little bit more for NCA samples than NGA series. For the activated with KOH samples the highest amount of nitrogen is for the sample of 1NCA-800 (0.72 wt.%). As aforementioned, the proper surface area, pore volume, and nitrogen content can all have a positive impact on increasing the capacitance of the electrode. The nitrogen content affecting capacitance is, as it has been reported that nitrogen atoms are electrochemically active due to being electron-rich [28,29].

The results of the X-ray powder diffraction analysis are shown in Figure S3(a,b). Figure S3(a) shows the results

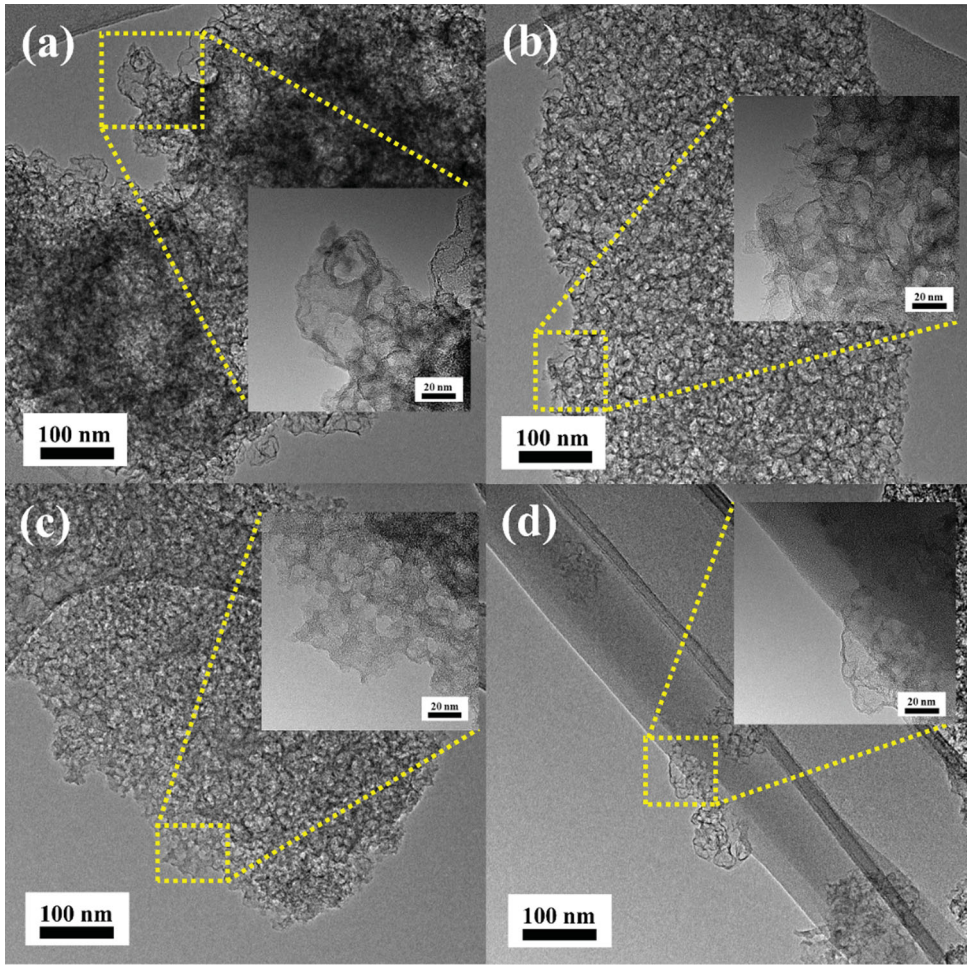

Figure 1. HRTEM images of: (a) 1NC, (b) 2NC, (c) 1NG, and (d) 2NG.

for materials obtained from natural algae before activation with two characteristic peaks at 24.1° and 43.3° associated with overlapping aromatic structure from graphite as graphene layers. Figure S3(b) shows the results for materials obtained from gelatine before and after activation with the same two characteristic peaks which indicate that before activation we have more ordered crystallographic structure than after activated materials. The materials before activation have a structure consisting of several layers of stacked graphene sheets. The broad peak at the angle two theta value from 20 to 25° can be attributed to the small dimensions of the crystallites, which are perpendicular to the graphene sheets [30,31].

The Raman spectra shown in Figure S3(c,d) indicate that there are three characteristic bands for graphene (D, G, and 2D-band) in all samples before and after activation. The D-band is responsible for the sp^3 hybrid structure of defining defects in the disordered carbon structure, while the G-band is responsible for the sp^2 hybrid structure of carbon of highly ordered graphite layers [32].

4.2. Electrochemical performance for a three-electrode configuration with neutral electrolyte

The CV profiles of the carbon materials in the neutral electrolyte (0.2 M K_2SO_4) are presented in Figure 3(a). It can be seen that the highest density current was achieved for both 1NCA-800 and 1NGA-800 electrode materials and that each curve shape indicates energy storage through an EDL rather than through pseudocapacitance. However, after several GCD cycles were performed, it can be observed that each electrode material is characterized by an increasing capacitance value, probably related to the activation processes due to electrolyte ion intercalation. On the basis of the three-electrode measurements, it can be said that after 100 GCD cycles, carbon materials are characterized by an enhanced capacitance (Figure 3(b)).

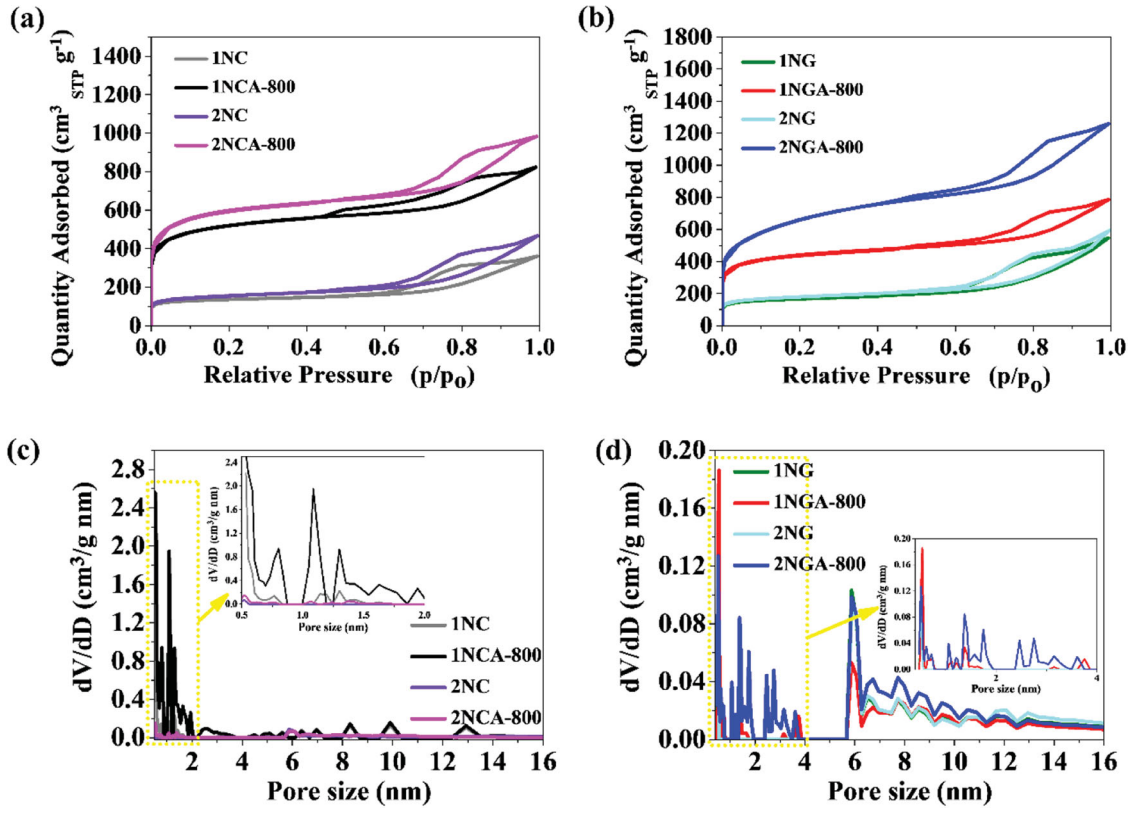

Figure 2. (a,b) Adsorption–desorption isotherms of N_2 measured at −196°C on porous carbon materials. (c,d) Pore size distributions (PSDs) were obtained by the NLDFT method.

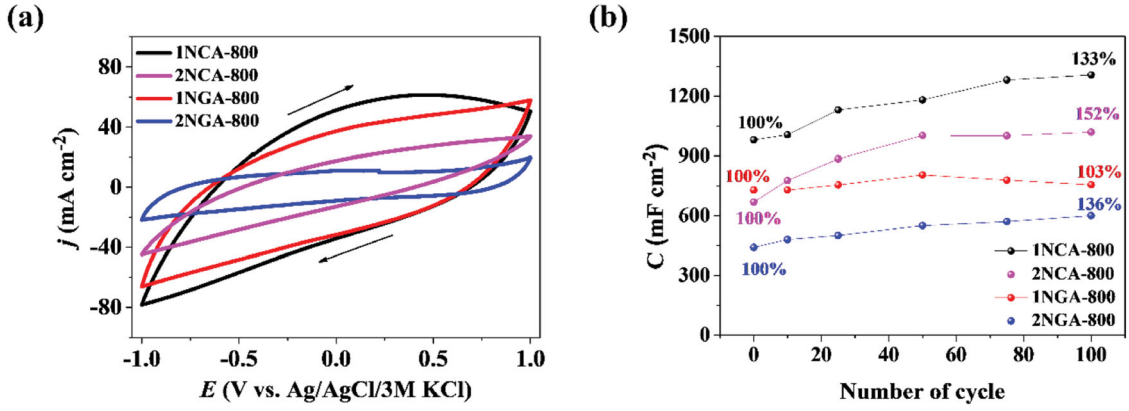

Figure 3. (a) Cyclic voltammetry curves recorded for carbon materials in 0.2 M K_2SO_4 (at a scan rate of $v = 50\,mV\,s^{-1}$) and (b) areal capacitance calculated on the basis of 100 galvanostatic charge/discharge cycles for carbon materials at a current density $j = 3\,mA\,cm^{-2}$.

4.3. Electrochemical performance of a two-electrode configuration with neutral electrolyte

In order to evaluate the long-term performance of the analyzed materials, 1000 GCD cycles were performed in a two-electrode configuration in 0.2 M K_2SO_4 with the carbon materials deposited onto graphite foil. In Figure 4, the specific capacitance for 1000 cycles for each electrode material is shown together with the inset presenting chronopotentiometry curves before and after the GCD test. More detailed capacitance results are shown in Table S2 in the Supplementary Information. As shown in Figure 4, the highest capacitance was obtained for the 1NCA-800 electrode material, which is consistent with the results obtained in three-electrode measurements. However, it is also characterized by the lowest capacitance retention value, though it is considerably high. The most promising capacitance retention can be distinguished for the 2NGA-800 carbon material, but in this case, specific capacitance was the lowest. Worth noting is the fact that the 1NGA-800 electrode material was characterized

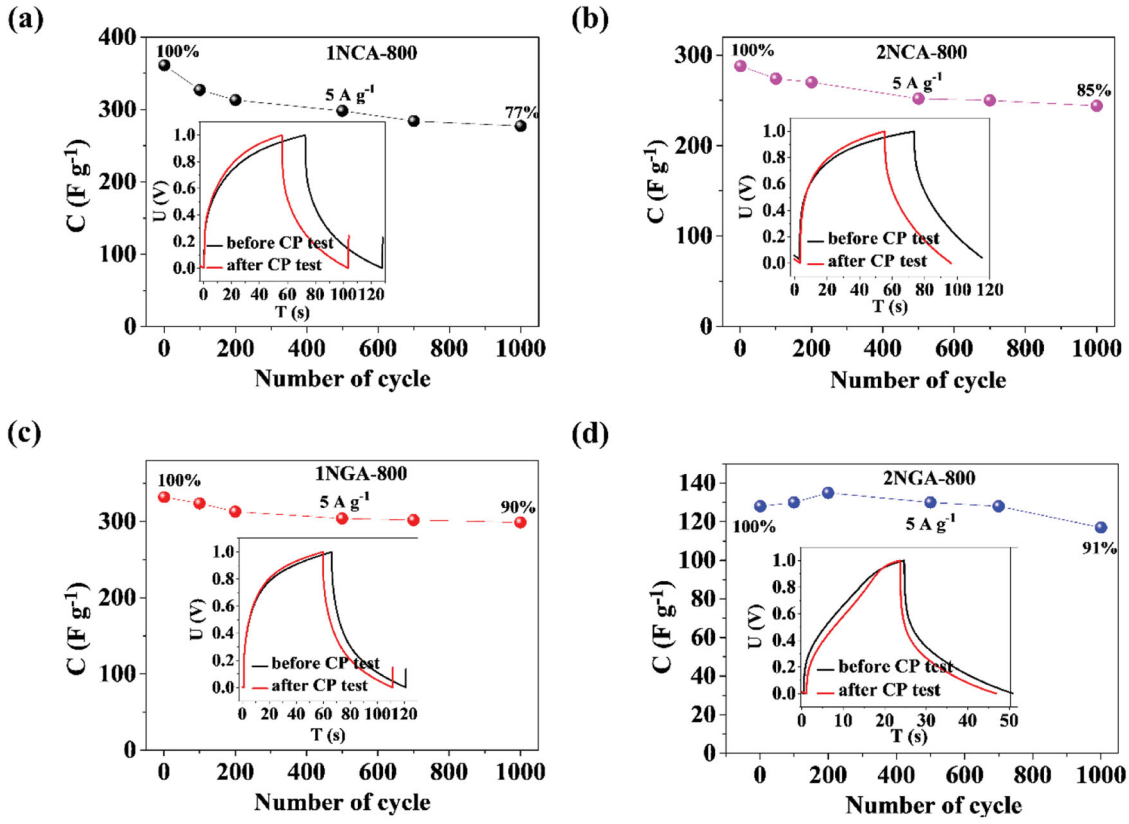

Figure 4. Specific capacitance plotted as a function of the number of GCD cycles for (a) 1NCA-800, (b) 2NCA-800, (c) 1NGA-800, and (d) 2NGA-800 (insets: GCD curves before and after charge/discharge tests recorded at a current density of 5 A g^{-1}) measured in 0.2 M K_2SO_4 electrolyte.

by both considerably high capacitance retention and high specific capacitance value, thus presenting possibly the best overall electrochemical performance. The highest capacitance, equal to 361 F g^{-1} at current density of 5 A g^{-1}, was determined for 1NGA-800 sample with high accessible surface area of 1642 m^2 g^{-1}. Furthermore, an analysis was performed regarding physicochemical properties and elemental composition, and their relation to the electrochemical measurements. When comparing the results from Table S1 in the Supplementary Information, it can be seen that higher capacitance values were obtained with increasing nitrogen content in the sample, which is consistent with a number of literature reports [33–36].

Moreover, it can be observed that the materials with the highest specific surface area (2NCA-800 and 2-NGA-800) are characterized by reduced capacitive properties, which indicate that a common statement that higher BET specific surface area contributes to higher capacitance values, is not always true. Those materials also have a larger micropore surface, which confirms that a large specific surface area does not necessarily mean an improved capacitance. Moreover, materials with moderate micropore volumes (1NCA-800 and 1NGA-800) result in enhanced electrochemical properties, whereas too small and too high volume is not beneficial and a clear correlation may be seen. Finally, it may be concluded that the total (%) contribution of micro- and mesopores may have some influence on capacitance retention, as the results indicate that their ratio of equal contribution (1:1) results in the highest capacitance retention, and with the progressive domination of micropores, the capacitance retention decreases. It is known that mesopores play a crucial role in energy storage processes due to their fast ion transport and charge storage ability [37,38]. The capacity variation at different discharge current densities (Figure S4 in the Supplementary Information) reveals that the supercapacitor device based on the N-doped carbon materials has a small internal resistance, which is beneficial for high power discharge in practical applications. It can be observed on the Ragone plot, which presents the power density and energy density of the device at different current densities, that the energy density value is comparable with the reference values (which are presented in Table S3 in the Supplementary Information). The results are presented in Figure 5(a) and they are consistent with the results above, namely both 1NCA-800 and 1NGA-800 are characterized by the most

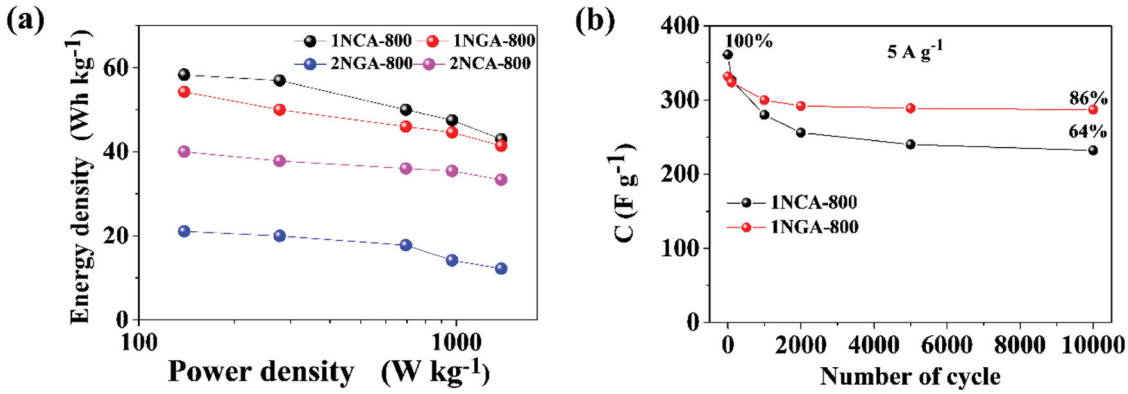

Figure 5. (a) Ragone plots for carbon materials in symmetric supercapacitors measured in 0.2 M K_2SO_4 electrolyte and (b) specific capacitance plotted as a function of the number of GCD cycles of 1NCA-800 and 1NGA-800 for 10,000 cycles.

promising properties for application in supercapacitors. The comparison of the overall electrochemical performance for the studied carbon materials is presented in Table S3 in the Supplementary Information, together with literature reports on carbon electrode materials. Multiple charge–discharge cycles (10,000 cycles) were performed in a two-electrode configuration for N-APC-800 and N-APC-900 in order to examine the stability of symmetric supercapacitors (Figure 5(b)) made for two types of the carbon materials (the best). The capacitance retention between the 1st and the 10,000th chronopotentiometry cycle was equal to 86% for 1NGA-800 and 64% for 1NCA-800. It is noteworthy that the decrease of the capacitance is the highest at the beginning of the charge–discharge tests, and then the capacitance stabilized after approximately 1000 cycles for 1NGA-800 and 2000 cycles for 1NCA-800. This means that the capacitance drop is related to some irreversible reactions on the material surface.

Moreover, the areal and volumetric capacitance was also calculated based on the GCD curves. The thickness of the layers was 29 and 21 μm for 1NCA-800 and 1NGA-800, respectively, which was estimated using the DektakXT profilometer. The 1NCA-800 exhibits areal and volumetric capacitance of 498 mF cm^{-2} and 17 F cm^{-3}, and the 1NGA-800-based supercapacitor shows 602 mF cm^{-2} and 28 F cm^{-3}, respectively (after 5000 cycles). The results of the areal and volumetric capacitive performance of the doped carbon-based supercapacitors have been included in the Supplementary information (see Figure S5). Both materials in the symmetric supercapacitor system were also characterized by a quite high-reaching coulombic efficiency during multiple cycles (Figure S6).

Figure S7 shows the electrochemical impedance spectra recorded for the 1NCA-800 and 1NGA-800-based symmetric supercapacitors at an open circuit potential (in a frequency range from 20 kHz to 1 Hz). In the high-frequency region, which represents the charge transfer resistance at the electrode–electrolyte interface, no semicircle was observed. On the other hand, the decreased slope in the low-frequency region indicates that there is a deviation from capacitive to pseudocapacitive behavior A small diameter or the absence of the semicircle indicates the small charge transfer resistance due to the porous structure of the materials [39,40].

A voltage leakage test was carried out for the selected electrode material (1NGA-800), as well, by charging the constructed supercapacitor with a current density of 2 A g^{-1} at 1 V of operating voltage. In the next step, open circuit potential was measured for about 500 s, and finally, a discharge with a current of 2 A g^{-1} was performed. As can be seen, the potential has not changed significantly (only by about 6%) during the OCP measurement and maintained the prior value, indicating good stability of the electrode material under charging conditions (see Figure S8).

5. Conclusion

In summary, nitrogen-doped porous carbons with high surface areas were prepared from gelatine and green algae—inexpensive, environmentally friendly, and renewable precursor. The investigated carbon electrodes with a low nitrogen content show that textural parameters are crucial factors influencing the samples' capacitance values. The carbon's BET surface area reached 2270 m^2 g^{-1} with a nitrogen content of 0.52 wt.%. The beneficial effect of nitrogen being substituted for carbon in the carbon layer is connected with enhancing the conductivity of the materials and increasing the active surface area accessible to the electrolyte by improving the wettability of the electrodes. Moreover, it also exhibits an attractive performance rate (after 10k cycles) in that the specific capacitance remains 86% (287 F g^{-1}) at a

current density of 5 A g^{-1}. The superior capacitive performance and low-cost and facile fabrication method of the nanoporous activated carbon electrode make it a very promising candidate for SCs applications. These results might be attributed to the unique structural and compositional features of materials, such as high specific area, desirable pore size distribution and sufficient electrochemically active sites.

Disclosure statement

No potential conflict of interest was reported by the author(s).

Funding

This work was carried out as a result of the research project no. LIDER/32/0116/L-9/17/NCBR/2018, financed by the National Centre for Research and Development.

References

[1] Deng X, Li J, Ma L, et al. Three-dimensional porous carbon materials and their composites as electrodes for electrochemical energy storage systems. Mater Chem Front. 2019;3(11):2221–2245.
[2] Jiang X, Chen Y, Meng X, et al. The impact of electrode with carbon materials on safety performance of lithium-ion batteries: a review. Carbon. 2022;191:448–470.
[3] Cui M, Meng X. Overview of transition metal-based composite materials for supercapacitor electrodes. Nanoscale Adv. 2020;2(12):5516–5528.
[4] Yadav S, Sharma A. Importance and challenges of hydrothermal technique for synthesis of transition metal oxides and composites as supercapacitor electrode materials. J Energy Storage. 2021;44:103295.
[5] Uppugalla S, Male U, Srinivasan P. Design and synthesis of heteroatoms doped carbon/polyaniline hybrid material for high performance electrode in supercapacitor application. Electrochim Acta. 2014;146:242–248.
[6] Shah SS, Alfasane MA, Bakare IA, et al. Polyaniline and heteroatoms–enriched carbon derived from pithophora polymorpha composite for high performance supercapacitor. J Energy Storage. 2020;30:101562.
[7] Yang Z, Xiang M, Zhu W, et al. Biomass heteroatom carbon/cerium dioxide composite nanomaterials electrode for high-performance supercapacitors. ACS Sustain Chem Eng. 2020;8(17):6675–6681.
[8] Gao K, Wang B, Tao L, et al. Efficient metal-free electrocatalysts from N-doped carbon nanomaterials: monodoping and Co-doping. Adv Mater. 2019;31(13):1805121.
[9] Lee WJ, Maiti UN, Lee JM, et al. Nitrogen-doped carbon nanotubes and graphene composite structures for energy and catalytic applications. Chem Commun. 2014;50(52):6818–6830.
[10] Hulicova-Jurcakova D, Seredych M, Lu GQ, et al. Combined effect of nitrogen-and oxygen-containing functional groups of microporous activated carbon on its electrochemical performance in supercapacitors. Adv Funct Mater. 2009;19(3):438–447.
[11] Gorgulho HF, Gonçalves F, Pereira MFR, et al. Synthesis and characterization of nitrogen-doped carbon xerogels. Carbon. 2009;47(8):2032–2039.
[12] Horikawa T, Sakao N, Sekida T, et al. Preparation of nitrogen-doped porous carbon by ammonia gas treatment and the effects of N-doping on water adsorption. Carbon. 2012;50(5):1833–1842.
[13] Wang X, Wang W, Qin R, et al. Defluorination-assisted heteroatom doping reaction with ammonia gas for synthesis of nitrogen-doped porous graphitized carbon. Chem Eng J. 2018;354:261–268.
[14] Zhang J, Yang Z, Wang X, et al. Homogeneous sulphur-doped composites: porous carbon materials with unique hierarchical porous nanostructure for super-capacitor application. RSC Adv. 2016;6(88):84847–84853.
[15] Deng Y, Ji Y, Wu H, et al. Enhanced electrochemical performance and high voltage window for supercapacitor based on multi-heteroatom modified porous carbon materials. Chem Commun. 2019;55(10):1486–1489.
[16] Ilnicka A, Lukaszewicz JP. Alternative synthesis method for carbon nanotubes. Small. 2019;15(51):1904132.
[17] Kamedulski P, Zielinski W, Nowak P, et al. 3D hierarchical porous hybrid nanostructure of carbon nanotubes and N-doped activated carbon. Sci Rep. 2020;10(1):1–11.
[18] Zielinski W, Kamedulski P, Smolarkiewicz-Wyczachowski A, et al. Synthesis of hybrid carbon materials consisting of N-doped microporous carbon and amorphous carbon nanotubes. Materials. 2020;13(13):2997.
[19] Zhou H, Yang H, Yao S, et al. Synthesis of 3D printing materials and their electrochemical applications. Chin Chem Lett. 2021;33(8):3681–3694.
[20] Zhou H, Zheng S, Guo X, et al. Ordered porous and uniform electric-field-strength micro-supercapacitors by 3D printing based on liquid-crystal V_2O_5 nanowires compositing carbon nanomaterials. J Colloid Interface Sci. 2022;628:24–32.
[21] Bai Y, Liu C, Chen T, et al. MXene-copper/cobalt hybrids via lewis acidic molten salts etching for high performance symmetric supercapacitors. Angew Chem. 2021;133(48):25522–25526.
[22] Zhou H, Cao W, Sun N, et al. Formation mechanism and properties of NiCoFeLDH@ ZIF-67 composites. Chin Chem Lett. 2021;32(10):3123–3127.
[23] He C, Liang J, Zou Y-H, et al. Metal-organic frameworks bonded with metal N-heterocyclic carbenes for efficient catalysis. Natl Sci Rev. 2022;9(6):nwab157.
[24] Ilnicka A, Skorupska M, Tyc M, et al. Green algae and gelatine derived nitrogen rich carbon as an outstanding competitor to Pt loaded carbon catalysts. Sci Rep. 2021;11(1):1–13.
[25] Salitra G, Soffer A, Eliad L, et al. Carbon electrodes for double-layer capacitors I. Relations between ion and pore dimensions. J Electrochem Soc. 2000;147(7):2486.
[26] Yamada Y, Tanaike O, Liang T-T, et al. Electric double layer capacitance performance of porous carbons prepared by defluorination of polytetrafluoroethylene with potassium. Electrochem Solid-State Lett. 2002;5(12):A283.
[27] Yoon S, Lee J, Hyeon T, et al. Electric double-layer capacitor performance of a new mesoporous carbon. J Electrochem Soc. 2000;147(7):2507.

[28] Frackowiak E. Carbon materials for supercapacitor application. Phys Chem Chem Phys. 2007;9(15):1774–1785.
[29] Rufford TE, Hulicova-Jurcakova D, Zhu Z, et al. Nanoporous carbon electrode from waste coffee beans for high performance supercapacitors. Electrochem Commun. 2008;10(10):1594–1597.
[30] Zgrzebnicki M, Nair V, Mitra S, et al. N-doped activated carbon derived from furfuryl alcohol–development of porosity, properties, and adsorption of carbon dioxide and ethene. Chem Eng J. 2022;427:131709.
[31] Yoshizawa N, Maruyama K, Yamada Y, et al. XRD evaluation of CO_2 activation process of coal-and coconut shell-based carbons. Fuel. 2000;79(12):1461–1466.
[32] Liu Y, Luo X, Zhou C, et al. A modulated electronic state strategy designed to integrate active HER and OER components as hybrid heterostructures for efficient overall water splitting. Appl Catal B. 2020;260:118197.
[33] Chen LF, Huang ZH, Liang HW, et al. Bacterial-cellulose-derived carbon nanofiber@ MnO_2 and nitrogen-doped carbon nanofiber electrode materials: an asymmetric supercapacitor with high energy and power density. Adv Mater. 2013;25(34):4746–4752.
[34] Ilnicka A, Skorupska M, Szkoda M, et al. Combined effect of nitrogen-doped functional groups and porosity of porous carbons on electrochemical performance of supercapacitors. Sci Rep. 2021;11(1):1–11.
[35] Zhao J, Lai H, Lyu Z, et al. Hydrophilic hierarchical nitrogen-doped carbon nanocages for ultrahigh supercapacitive performance. Adv Mater. 2015;27(23):3541–3545.
[36] Sun L, Wang L, Tian C, et al. Nitrogen-doped graphene with high nitrogen level via a one-step hydrothermal reaction of graphene oxide with urea for superior capacitive energy storage. RSC Adv. 2012;2(10):4498–4506.
[37] Li Y, Zhang D, Zhang Y, et al. Biomass-derived microporous carbon with large micropore size for high-performance supercapacitors. J Power Sources. 2020;448:227396.
[38] Zhang Q, Han K, Li S, et al. Synthesis of garlic skin-derived 3D hierarchical porous carbon for high-performance supercapacitors. Nanoscale. 2018;10(5):2427–2437.
[39] Chen GZ. Linear and non-linear pseudocapacitances with or without diffusion control. Prog Nat Sci: Mater Int. 2021;31(6):792–800.
[40] Lu C, Yang L, Yan B, et al. Nitrogen-doped Ti_3C_2 MXene: mechanism investigation and electrochemical analysis. Adv Funct Mater. 2020;30(47):2000852.